Analytic design of multiple-axis, multifocal diffractive lenses

Pedro J. Valle* and Manuel P. Cagigal

Dept. de Física Aplicada, Universidad de Cantabria, Los Castros S/N 39005 Santander, Spain
**Corresponding author: vallep@unican.es*

Received November 28, 2011; revised January 10, 2012; accepted January 26, 2012;
posted January 27, 2012 (Doc. ID 159041); published March 15, 2012

In this Letter, we introduce an analytic procedure for designing diffractive lenses using the combination of wavefronts aberrated by Zernike polynomials. We show how to design amplitude-only, phase-only, continuous, and binary lenses providing equivalent results. As an example we apply it to the design of a multiple-axis, multifocal lens. The number of foci and their positions can be easily controlled. Theoretical predictions have been experimentally confirmed. The main advantage of this procedure is that, because it is simple and intuitive, it can be used successfully for the design of complex lenses. © 2012 Optical Society of America

OCIS codes: 050.1965, 110.4190, 110.6880, 170.6900.

Diffractive lenses are optical elements widely used nowadays in numerous application areas, so to introduce a simple and intuitive designing method is of great interest. Many approaches have been carried out to design multifocal lenses [1], extended-focal-depth lenses [2] or variable-focal-length devices [3]. An interesting and extensive review of diffractive lens design and applications has been addressed by M. A. Golub [4]. Although different approaches have been carried out for designing diffractive lenses, our goal is to introduce an analytic procedure based on the use of wavefronts aberrated by simple Zernike polynomials. We apply it to design a multiple-axis, multifocal lens. The procedure allows us an easy control of the foci number, their relative orientation and separation, and even their shape. We also show that amplitude-only, phase-only, continuous, and binary lenses give basically the same results. An advantage of these lenses is to provide simultaneous images of many planes using only one imaging system and one image detector.

A simple experimental setup is used to confirm that the theoretically introduced diffractive lenses are capable of acting as off-axis multifocal lenses. We have seen that a particular proposed lens provides three foci axially and transversally distributed. In addition, this lens is able to focus different object planes in different detector regions.

We will work within the framework of the scalar diffraction theory. Let us consider a general complex pupil function $P(\rho,\theta) = A(\rho,\theta)\exp[i\phi(\rho,\theta)]$, where ρ and θ are the normalized radial and polar coordinates over the optical-system pupil plane. A converging, monochromatic, spherical wavefront passing through the center of the pupil produces wave amplitude in the focal region given by [5]

$$U(v,\phi,u) = \int_0^{2\pi}\int_0^1 P(\rho,\theta)\exp[iv\rho\,\cos(\theta-\phi) + \frac{i}{2}u\rho^2]\rho\mathrm{d}\theta\mathrm{d}\rho, \quad (1)$$

where v and u are radial and axial dimensionless optical coordinates with origin at the geometrical focus, given by $v = k\mathrm{NA}r$ and $u = k\mathrm{NA}^2 z$. NA is the numerical aperture; $k = 2\pi/\lambda$; and r, φ, and z are the cylindrical coordinates with origin at the geometrical focus (Cartesian coordinates in the focal region are $x = r\cos(\varphi)$, $y = r\sin(\varphi)$, and z). A phase pupil containing the tilt Zernike polynomial, $P(\rho,\theta) = \exp[i\alpha\rho\cos(\theta)]$, produces a focus displacement from the optical axis in the x direction proportional to α. Then, the pupil $P(\rho,\theta) = \exp[i\alpha\rho\cos(\theta)] + \exp[-i\alpha\rho\cos(\theta)]$ will provide two foci with the same energy at distances proportional to $\pm\alpha$. The pupil function to obtain a number of foci pairs will be

$$P(\rho,\theta) = \mathrm{offset} + \sum_m c_m\cos[\alpha_m\rho\cos(\theta-\phi_m)]. \quad (2)$$

Coefficients c_m allow controlling the relative light intensity of the corresponding foci pair and φ_m the foci pair orientation. The *offset* introduced into Eq. (2) to force the pupil to be an amplitude-only function [by setting $P(\rho,\theta) \geq 0$] produces an additional central focus. Figure 1(a) sketches the case for $m = 1$ and $\varphi_1 = 0$ in Eq. (2) that corresponds to three foci (points a, b, and c) along the x axis.

To obtain foci pairs distributed along the z axis, we will use the defocus Zernike polynomial as follows: $P(\rho,\theta) = \exp(i\beta\rho^2) + \exp(-i\beta\rho^2)$. A number of foci pairs along the z axis at distances from the origin proportional to $\pm\beta_m$ can be obtained using the pupil function:

$$P(\rho,\theta) = \mathrm{offset} + \sum_m c_m\cos(\beta_m\rho^2). \quad (3)$$

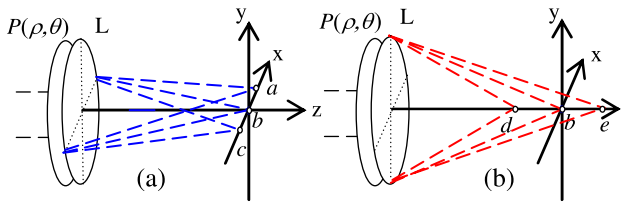

Fig. 1. (Color online) (a) Three focal points (a,b,c) placed along the x axis as a result of using the pupil function given by Eq. (2) for $m = 1$ and $\varphi_1 = 0$. (b) Three focal points (d,b,e) placed along the z axis as a result of using the pupil function given by Eq. (3) for $m = 1$.

The *offset* is again introduced to get an amplitude-only pupil. Figure 1(b) sketches the case of three axial foci (points b, d, and e) obtained for $m = 1$ in Eq. (3).

Combining Eqs. (2) and (3) we obtain

$$P(\rho,\theta) = \text{offset} + \sum_m c_m \cos[\alpha_m \rho \cos(\theta - \phi_m) + \beta_m \rho^2]. \quad (4)$$

Eq. (4) allows imaging pairs of planes distributed along the z axis, pairs of tilted planes, or a combination of both types. This example of combination of the two first Zernike polynomials can be easily extended to spherical aberration and astigmatism by addition of the corresponding Zernike polynomial into the argument of the cosine functions in Eq. (4).

The procedure shown here not only allows making multifocal lenses but also more complex light intensity distribution. For example, multiplying Eq. (2) by the function $J_1(\gamma\rho)/\rho$ (where J_1 is the first-order Bessel function), we obtain a series of top-hat intensity profiles uniformly distributed over the image plane, which, for a proper γ value, performs like a diffractive diffuser [6]. What is more, when working with polychromatic light, achromatic and apochromatic foci can be obtained with only selecting the proper β_m value in Eq. (3) for every wavelength used [7].

The amplitude-only diffractive lenses here proposed are absorbing elements, and this could be a drawback in some applications. In order to get phase-only lenses, the following pupil function is proposed:

$$P(\rho,\theta) = \exp\left[i \sum_m c_m \cos(\alpha_m \rho \cos(\theta - \varphi_m) + \beta_m \rho^2) \right]. \quad (5)$$

The first two terms of the expansion of the exponential in Eq. (5) reproduce the results given by Eq. (4) with only setting offset = 1. The remaining terms create a series of extra foci pairs with negligible intensity compared to those of the main foci. A rigorous explanation of this can be found in [1].

Manufacturing continuous pupil functions may be difficult and expensive; hence we have developed binary functions providing the same foci as continuous ones. A binary pupil $\text{BP}(\rho,\theta)$ can be obtained by assigning a transmittance value equal to 1 at the points where the function of Eq. (4) is above a threshold and transmittance 0 to others. We have verified that, apart from some extra foci with negligible intensity, continuous and binary lenses provide the same light distribution. Binary phase lenses can also be derived by substituting the exponent in Eq. (5) by $\sigma\text{BP}(\rho,\theta)$, where σ is a parameter that ranges from 0 to π. These lenses provide the same foci as continuous ones, although the relative intensity between foci depends on the σ value as well. In particular, for $\sigma = \pi$ the central focus disappears.

To check proposed diffractive lenses we used the experimental setup shown in Fig. 2(a). The light source consists on a He-Ne laser (632 nm), which is spatially filtered (SF) and collimated using a lens (CL, 60 cm focal length). The plane wavefront so obtained is reflected by a Hamamatsu spatial light modulator (SLM) model PPM X8267 that can work in amplitude-only or phase-only modes.

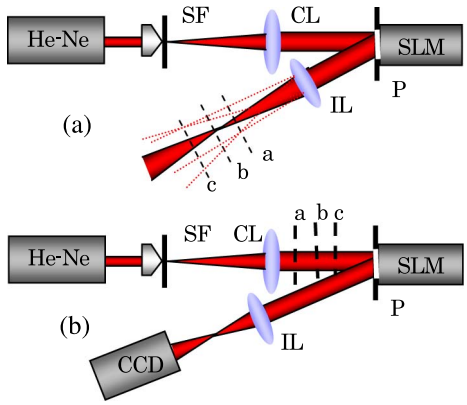

Fig. 2. (Color online) (a) Experimental setup used for checking the different foci and (b) that used for checking the diffractive lens capability of simultaneously imaging objects placed at different distances.

A 6 mm diameter pupil (P) was set over the modulator surface at the front focal plane of the imaging lens (IL, 40 cm focal length).

We have checked that the diffraction efficiency of our lenses for the first-order foci ranges from 6.25% for amplitude continuous pupils up to 40% for phase binary pupils, as expected from the grating theory.

We have checked that both amplitude-only and phase-only diffractive lenses provide the same spatial foci distribution, although we prefer phase-only filters because of their energy efficiency. The phase-only profile used in our experiment is given by

$$P(\rho,\theta) = \exp\{i \cos[\alpha\rho \cos(\theta) + \beta\rho^2]\}. \quad (6)$$

A grey-level version of the phase distribution given by Eq. (6) is shown in Fig. 3(d). For the particular α and β values used for creating the pupil, we obtained a central focal point at (0, 0, 0) and two additional foci placed at

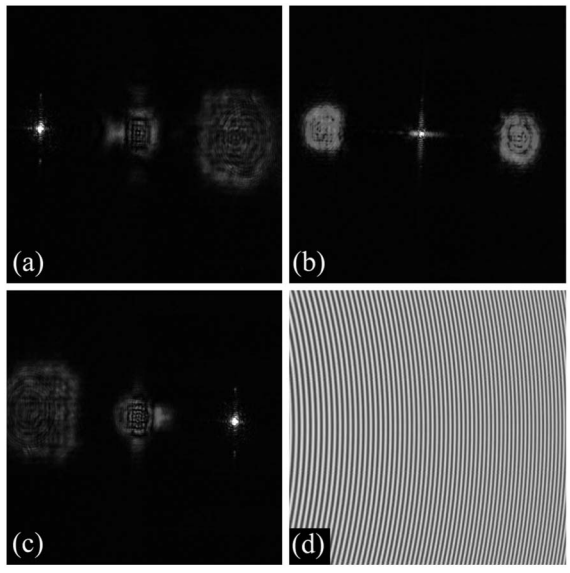

Fig. 3. (a–c) Light intensity distribution at the focal planes a, b and c shown in Fig. 2(a). (d) Phase-only pupil function represented as a grey-level function.

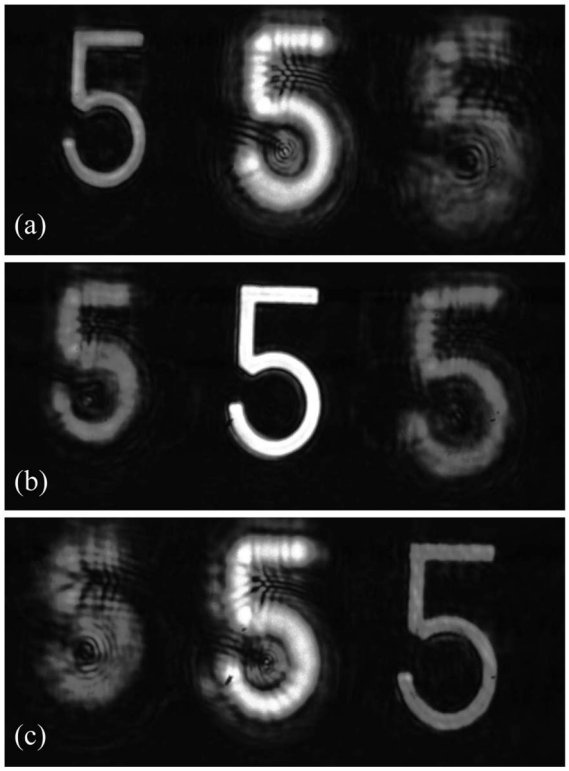

Fig. 4. Images obtained in the CCD when the object was placed at three different positions (a, b, and c).

positions (–2, 0, –10) and (2, 0, 10). (Coordinates in the focal region $x = r\ \cos(\varphi)$, $y = r\ \sin(\varphi)$, and z are in mm)

Figure 3(a) shows the light intensity distribution in a plane placed 10 mm before the IL back focal plane, and it consists of a clear focus and two defocused light spots. The light distribution at a plane placed 10 mm after the IL focal plane is shown in Fig. 3(c), and it is symmetrical with respect to that of Fig. 3(a), as expected. Figure 3(b) shows the light distribution at the IL focal plane, where in addition to the expected central focus there also also appear two lateral spots corresponding to diffuse light coming from and going to the other two foci. As an example of application, the shape of the incoming wavefront can be reconstructed from the intensity of the two lateral spots following the procedure used in the curvature wavefront sensors [8].

To test the ability of the previous lens to image objects, we carried out an experiment using the setup of Fig. 2(b). A CCD camera was sited at a fixed position after the IL to register the image series. We placed an object, consisting of a mask containing the number 5, along the optical axis at three distances from the IL [a, b, c in Fig. 2(b)]. Figure 4 shows that three different images of the original object are always present. When the number 5 is placed at axial position (a), the image on the left in Fig. 4(a) is the only one clearly focused. When the object is at the axial position (b), the central image is focused [Fig. 4(b)]; and when the object is at the axial position (c), only the right image is focused [Fig. 4(c)]. In this case the central image has more intensity than the others, but relative intensity can be controlled using the proper coefficients in the exponent of Eq. (5). In Fig. 4, it can also be seen that the sizes of the three images are different, which is consequent with the fact that the three objects are placed at different distances from the imaging lens.

In our experimental setup we used a small numeral aperture system (NA = 0.015) and a diffractive lens producing a small additional defocus. This allowed us to compare the size and the position of the images coming from the different axial planes. Our results basically coincide with those obtained using lenses designed by phase diversity [9], which supports the conclusion that our procedure works properly. Particularly interesting applications for this kind of lenses are reading in multilayer optical disc storage [10] or in layered peptide array systems [11].

On the other hand, α and β values in Eq. (6) can be used to control the distance between images and their relative size, respectively, as previously mentioned. In particular, setting $\beta = 0$ [the case sketched in Fig. 1(a)], the lens provides three images corresponding to three different observation directions. This lens could be used to convert a single-axis microscope objective into a multiple-axes one in a cheap and simple way [12] or to improve three-dimensional imaging [13].

In conclusion, we have shown a simple procedure for designing multiple-foci diffractive lenses based on the combination of aberrated wavefronts on the base of the Zernike polynomials. We have checked that amplitude-only and phase-only, in both continuous and binary versions, provide equivalent spatial foci distributions. A simple experiment has been carried out to confirm the theoretical predictions. The main advantage of the procedure introduced here is that it is simple, intuitive, and allows designing complicated (mono- or polychromatic) elements in an easy way.

This research was supported by the Ministerio de Ciencia e Innovación under project AYA2010-19506.

References

1. P. J. Valle, J. E. Oti, V. F. Canales, and M. P. Cagigal, Opt. Commun. **272**, 325 (2007).
2. A. García, S. Bará, M. Gómez García, Z. Jaroszewicz, A. Kolodziejczyk, and K. Petelczyc, Opt. Express **16**, 18371 (2008).
3. P. J. Valle, V. F. Canales, and M. P. Cagigal, Opt. Express **18**, 7820 (2010).
4. M. A. Golub, Opt. Photon. News **15**, 36 (2004).
5. M. Born and E. Wolf, *Principles of Optics* (Cambridge University, 1999).
6. http://www.jenoptik-inc.com/microoptic-solutions/diffractive-optical-elements/diffractive-diffusers.html.
7. D. Faklis and G. M. Morris, Appl. Opt. **34**, 2462 (1995).
8. X. Fengjie, J. Zongfu, X. Xiaojun, and G. Yifeng, J. Opt. Soc. Am. A **24**, 3444 (2007).
9. P. M. Blanchard and A. H. Greenaway, Appl. Opt. **38**, 6692 (1999).
10. T. Ide, S. Kimura, E. Tatsu, T. Kurokawa, K. Watanabe, Y. Anzai, and T. Shintani, Appl. Opt. **49**, 2309 (2010).
11. R. Cohen, G. Gannot, M. Ben David, N. Sochen, and I. Gannot, Opt. Express **19**, 19822 (2011).
12. J. Swoger, J. Huisken, and E. H. K. Stelzer, Opt. Lett. **28**, 1654 (2003).
13. R. Martínez-Cuenca, H. Navarro, G. Saavedra, B. Javidi, and M. Martínez-Corral, Opt. Express **15**, 16255 (2007).